Chaos ARTICLE pubs.aip.org/aip/cha

Efficient driver-node selection for pinning control via second-order perturbations

Cite as: Chaos 36, 093150 (2026); doi: 10.1063/5.0351619
Submitted: 8 July 2026 · Accepted: 8 September 2026 ·
Published Online: 28 September 2026

View Online Export Citation CrossMark

Fatemeh Ghoreishian Amiri,[1] Fahimeh Nazarimehr,[1,a)] Sajad Jafari,[1,2] and Matjaž Perc[3,4,5,6,a)]

AFFILIATIONS

[1]Department of Biomedical Engineering, Amirkabir University of Technology (Tehran Polytechnic), Tehran, Iran
[2]Health Technology Research Institute, Amirkabir University of Technology (Tehran Polytechnic), Tehran, Iran
[3]Faculty of Natural Sciences and Mathematics, University of Maribor, Koroška cesta 160, 2000 Maribor, Slovenia
[4]Community Healthcare Center Dr. Adolf Drolc Maribor, Ulica talcev 9, 2000 Maribor, Slovenia
[5]Department of Physics, Kyung Hee University, 26 Kyungheedae-ro, Dongdaemun-gu, Seoul 02447, Republic of Korea
[6]University College, Korea University, 145 Anam-ro, Seongbuk-gu, Seoul 02841, Republic of Korea

[a)]**Authors to whom correspondence should be addressed:** f_nazarimehr@aut.ac.ir and matjaz.perc@gmail.com

ABSTRACT

Driver-node selection is a fundamental problem in the pinning control of complex networks, where the aim is to identify a small set of nodes whose external control can most effectively steer the collective dynamics of the network. Driver nodes are typically selected sequentially, and greedy optimization serves as the standard benchmark for such sequential methods since it produces near-optimal node sets. However, this level of accuracy comes at a computational cost that becomes prohibitive for large networks. In this work, we propose a second-order perturbation framework that overcomes this limitation by estimating the shift in the smallest eigenvalue of the network Laplacian, the quantity that governs the stability of the pinned network, using second-order perturbation theory. Consequently, the proposed method reduces the computational complexity of driver-node selection from $O(N^5)$ in conventional greedy schemes to $O(N^4)$, enabling efficient and scalable selection in large-scale networks. Extensive simulations across diverse network topologies, including small-world, scale-free, and random networks, demonstrate that the proposed method consistently outperforms standard centrality-based heuristics. It achieves performance comparable to optimal greedy benchmarks, while offering substantially higher computational efficiency. The proposed framework thus provides a practical and scalable solution for the control of large complex networks, and more broadly, demonstrates the utility of higher-order perturbation analysis for node-ranking problems in network controllability.

Published under an exclusive license by AIP Publishing. https://doi.org/10.1063/5.0351619

28 September 2026 14:34:12

The efficient selection of driver nodes is a critical bottleneck in the pinning control of complex dynamical networks. While greedy algorithms provide high accuracy, their intensive computational requirements limit their applicability to large-scale systems. This paper proposes a scalable alternative based on a second-order perturbation theory to rank candidate nodes by approximating the sensitivity of the smallest Laplacian eigenvalue to diagonal perturbations induced by node pinning. The proposed method outperforms standard centrality-based heuristics and provides a substantial improvement in accuracy over the first-order perturbation method. By lowering the computational complexity from $O(N^5)$ to $O(N^4)$, the proposed approach offers an efficient alternative to greedy methods without sacrificing selection quality. It achieves a high level of accuracy in identifying critical driver nodes, comparable to that of computationally intensive greedy searches, thereby enabling effective control of large-scale networked systems with reduced computational demands.

I. INTRODUCTION

The ability to control complex networks is one of the main themes in research on dynamical systems and network theory.[1,2] The dynamical patterns observed in a system arise from the mutual influence between the network's topology and the governing laws that regulate interactions among its nodes.[3] Among various strategies for controlling complex networks, pinning control manipulates only a limited group of nodes so that the entire network eventually tracks a prescribed external reference signal.[4] Developing strategies that achieve effective network control

Published under an exclusive license by AIP Publishing

while minimizing resource usage has attracted significant attention in the literature.[1,5,6] This problem is significant for large-scale networks, such as those found in chemical processes,[7] biological networks,[8] and social systems.[9–11] To provide a comprehensive understanding of the current state of research, key contributions on pinning control and network synchronization are reviewed.

An essential application of pinning control lies in achieving network synchronization, where all nodes are steered toward a common target state. In complex network structures, synchronization plays a crucial role in processes observed in neuroscience and biological contexts.[12] Majhi *et al.*[13] examined how neuronal networks achieve synchrony, highlighting the roles of both dyadic and higher-order interactions in producing intricate spatiotemporal patterns in which synchronous and asynchronous dynamics appear simultaneously. Franović *et al.*[14] conducted research on neuronal networks with noisy excitability and showed that synchronization clusters emerge due to the combined effects of coupling delays, noise, and the inherent excitable dynamics of neurons. Investigations of coupled inhibitory neurons with synaptic delays have revealed that modifications to synaptic characteristics influence the likelihood of neurons achieving synchronized states within specific arrangements, indicating a progressive transition from anti-phase to in-phase coordination.[15] Positive interconnections among oscillators typically facilitate synchronization in phase alignment, leading to either complete synchrony in identical systems or partial phase coherence in diverse ones.[16] Acharya *et al.*[17] analyzed distance-type synchronization in conservative chaotic oscillators possessing axial symmetry and linked through a master–slave interaction. Their results showed that the oscillators synchronize into a synchronous state with a fixed phase offset dictated by the strength of the coupling. To address synchronization challenges in large-scale networks with time delays, Xu *et al.*[18] proposed an intermittent event-triggered control strategy. Their framework, utilizing both continuous and periodic sampling, leverages a generalized Halanay inequality and Lyapunov stability theory to derive synchronization criteria. The effectiveness of this approach was demonstrated through analytical results and a practical application in robot arm systems. Ye and colleagues[19] explored the parameter regimes that best facilitate synchronization in higher-order neural networks constructed from triplet motifs. Their work utilized the Dynamic Learning of Synchronization (DLS) approach, where connection weights are adjusted to modulate firing patterns. Along similar lines, Wu *et al.*[20] proposed a DLS-based scheme designed to secure robust synchronization in networks of nonlinear coupled systems. Their algorithm persistently updates the coupling weights between nodes, allowing the network to maintain synchronous behavior following adaptation. By employing the Master Stability Function (MSF), they confirmed that the DLS mechanism guides the system toward regions where synchronization is stable. Recent analyses based on the MSF have demonstrated that the arrangement of couplings, together with whether the interactions involve single or multiple node variables, plays a decisive role in determining the minimum coupling strength that guarantees stable synchrony.[21] Ding *et al.*[22] also applied the DLS method to achieve adaptive global and local synchronization. They examined the robustness of DLS under noisy conditions, showing that it maintained strong performance in weak noise environments.

In multilayered networks featuring mobile nodes, the synchronization dynamics, both within and between layers, are highly sensitive to parameters associated with mobility and coupling strengths. Notably, this synchronization can exhibit robustness against structural and dynamical perturbations.[23] In a study by Wang *et al.*,[24] the challenge of achieving pinning synchronization within impulsive Lur'e networks characterized by nonlinear and asymmetric couplings was addressed. Their proposed single pinning impulsive controller was designed to account for both synchronizing and desynchronizing impulses, leveraging the principles of average impulsive interval and gain. Utilizing the Lyapunov method, the researchers established rigorous conditions guaranteeing exponential synchronization even in the presence of hybrid impulses, with numerical simulations confirming the efficacy of their developed technique. Chen *et al.*[25] investigated synchronization in a 9D system composed of two identical memristive subsystems coupled via a memristor, focusing on how initial conditions influence synchronous behaviors. Synchronization in this system, which is highly sensitive to initial conditions, was theoretically confirmed through Lyapunov-based stability analysis. Xiao *et al.*[26] proposed a novel approach for synchronization control in stochastic networked systems using a hierarchy of polynomial Lyapunov functions. Their method unifies the design of distributed control protocols and synchronization guarantees through a convex sum-of-squares optimization framework.

Some studies have emphasized the theoretical foundations and mathematical principles of control, illustrating how network structure, node selection, and local controllers govern the stabilization, synchronization, and overall controllability of the system. It has been shown that complex systems encompass multiple stability regimes, spanning from marginal instability—where no stable state is attainable—to sensitive conditions, in which stability appears only within a narrow interval of the system's parameters.[27] Yildirim *et al.*[28] analyzed multiagent networks on directed graphs, addressing exogenous disturbances from misbehaving nodes. They introduced a proportional-integral feedback control strategy using a subset of driver nodes to ensure the network's input-to-state stability. Their graph-theoretical method allows the critical steady-state values of nodes to be determined without full knowledge of the Laplacian matrix. Pasqualetti *et al.*[29] tackled the dual problem of selecting optimal driver nodes and devising control inputs for state steering in networks. They introduced a metric for control complexity based on energy use. Additionally, they defined foundational energy-node trade-off limits, stemming from the system's dynamics (topology and edge weights). Finally, they presented an open-loop control method, merging graph partitioning for node identification with distributed optimal control for input design. Li *et al.*[30] addressed the challenge of ensuring structural controllability in multiplex networks by determining the smallest possible set of control or driver nodes. Using a graph-theoretic formulation, they showed that this selection task can be transformed into a minimum-cost flow optimization problem. Based on this insight, they designed an efficient algorithm capable of identifying the optimal driver nodes with polynomial computational complexity.

28 September 2026 14:34:12

Published under an exclusive license by AIP Publishing

Expanding on these theoretical frameworks, a significant body of research has emerged to address the critical bottleneck of identifying optimal driver-node sets for enhanced pinning control. Recognizing that node selection is a decisive factor in achieving global stability with minimal control effort, several studies have proposed diverse selection criteria ranging from structural heuristics to optimization-based frameworks. In this context, Liu *et al.*[31] leveraged matrix spectral theory to design a node-selection mechanism that evaluates the influence of pinned sites on the spectrum of the network Laplacian. By formulating an optimization problem geared toward enhancing synchronization capability, they employed eigenvalue perturbation tools to characterize the resulting spectral shifts. Alanis *et al.*[32] considered the task of identifying suitable control nodes in complex dynamical networks such that stability can be achieved with limited control energy and implementation effort. Since an exhaustive examination of all possible node subsets is computationally prohibitive in large nonlinear networks, they employed binary optimization techniques to identify a subset of nodes that can efficiently guide the network dynamics toward the zero equilibrium. In another contribution, Moradiamani *et al.*[33] tackled driver-set determination by adopting the eigenratio of the modified Laplacian as an optimization benchmark, aiming to expand the admissible coupling-strength interval for stable synchronization. To circumvent intensive combinatorial searches, they formulated a computationally tractable centrality index based on the spectral sensitivity of the Laplacian, enabling driver identification via merely a single matrix diagonalization. Focusing on directed topologies, Zhang *et al.*[34] introduced a quantitative index named control contribution to gauge nodal steering capabilities. This descriptor synthesizes a node's propensity to belong to a minimal driver configuration with its capacity to dictate the states of neighboring units. Addressing time-evolving systems, Qin *et al.*[35] designed a fast, real-time heuristic routine to track driver nodes across temporal graphs. Their theoretical and numerical assessments on both synthetic benchmarks and empirical datasets revealed that a substantial fraction of temporal links is superfluous for steering the network, whereas pathways characterized by high betweenness centrality prove indispensable for preserving controllability. In the context of restoring functional dynamics within oscillator ensembles, Bomela *et al.*[36] focused on pinpointing the most influential node to serve as a single pinning target. They devised an algebraic scheme centered on the Moore–Penrose pseudoinverse of the Laplacian, illustrating that the optimal target site can migrate as the control gain varies; consequently, distinct nodes emerge as dominant under weak interaction regimes compared with strong interaction regimes. In a related study, Zhang *et al.*[37] considered the problem of selecting the most effective driver nodes for accelerating synchronization in multi-agent networks with switching topologies. They established synchronization criteria under pinning control and introduced a selection scheme that guarantees the highest convergence rate in periodically switched systems. Their results further showed that, under certain assumptions, the optimal choice of driver nodes does not depend on the system matrix.

Hui *et al.*[38] examined the optimization of pinning-control schemes in large-scale complex networks by employing the minimum eigenvalue, λ_1, of the grounded Laplacian as an indicator of network controllability. Because the maximization of λ_1 constitutes an NP-hard optimization task, they proposed a filtering-based procedure for detecting the nodes that exert the greatest influence on this spectral quantity and for obtaining the best attainable λ_1 under a prescribed pinning budget. Their study introduced the notion of node-set importance, showing that the best driver-node configuration is not fixed but varies with the number of nodes selected for pinning. Along similar lines, Zhou *et al.*[39] considered the selection of a node subset in a connected network so as to maximize the smallest eigenvalue of the grounded Laplacian. Since this eigenvalue governs both the performance of pinning control and the convergence speed of leader–follower dynamics, its maximization provides a meaningful criterion for node placement. They established that the associated objective is monotonic, although it does not possess the submodularity property. To address the resulting computational difficulty, they first designed an iterative heuristic for sequential node selection and subsequently developed a scalable greedy approach that combines derivative matrices, eigenvalue perturbation analysis, and Laplacian solvers to achieve scalable node selection.

Despite these notable advances, the problem of identifying optimal driver nodes remains computationally demanding, particularly in large-scale networks where repeated spectral evaluations are required. In addition, although greedy and heuristic strategies can substantially improve efficiency, they still rely on sequential node updates and may become costly when the network size grows or when rapid repeated assessments are needed. These limitations motivate the development of a more systematic spectral approximation scheme that can retain the accuracy of eigenvalue-based selection while reducing computational overhead. In this paper, we, therefore, present a second-order perturbation framework for the systematic selection of driver nodes in pinning control.

The approach uses eigenvalue perturbation theory to approximate the effect of diagonal modifications of the Laplacian on its smallest eigenvalue, thereby providing a computationally efficient criterion for node selection. Unlike the conventional greedy algorithm, which requires repeated eigenvalue computations and scales poorly with network size, the proposed method achieves comparable accuracy with reduced computational cost. Through extensive experiments on networks with various topologies—including small-world, scale-free, and random models—the proposed method is shown not only to reduce computational burden while producing results comparable to those of the benchmark greedy strategy, making it a promising tool for large-scale network-controllability analysis. The remainder of this paper is structured as follows. Section II establishes the necessary theoretical groundwork. It begins by examining pinning control in complex networks, followed by a rigorous convergence analysis in pinning synchronization, and concludes with an overview of the first- and second-order perturbation theory. Section III introduces the proposed method, detailing the core algorithmic contributions. Section IV presents the results, offering a comprehensive evaluation of the proposed approach through extensive simulations. In Sec. V, a critical discussion on the implications of the findings and their broader context is provided. Finally, Sec. VI offers the conclusion, summarizing the key insights and outlining potential directions for future research.

28 September 2026 14:34:12

Published under an exclusive license by AIP Publishing

II. PRELIMINARIES

In this section, the fundamental concepts and control strategies relevant to this study are briefly reviewed.

A. Pinning control in complex networks

Pinning control is a widely used framework for stabilizing and steering the dynamics of complex networks toward a desired manifold or trajectory.[40] The central idea is that instead of applying control inputs to all nodes, only a small fraction of nodes—referred to as driver nodes or pinned nodes—are directly controlled,[41] while their influence propagates to the rest of the network through the coupling structure. In the pinning control framework, the dynamics of nodes are defined as

$$\dot{x}_i = F(x_i) - c\sum_{j=1}^{N} l_{ij}\Gamma x_j - d_i\Gamma(x_i - s), \quad i = 1, \ldots, N, \tag{1}$$

where $x_i = (x_{i1}, x_{i2}, x_{i3}, \ldots, x_{im}) \in \mathbb{R}^m$ represents the m-dimensional state vector associated with node i, capturing its underlying dynamics. The term $F(x_i)$ characterizes the local dynamics at that node. The entry l_{ij} corresponds to the (i, j)th component of the Laplacian matrix L, while c denotes the coupling intensity. $d_i \geq 0$ specifies the control input applied at node i; a node selected as a driver receives gain $d_i = d$, whereas all other nodes have $d_i = 0$. The scalar d denotes the control gain. The aim is to drive the network toward a synchronized configuration or a prescribed manifold s.

To assess the stability of the stationary state s, Eq. (1) is linearized about s, which results in

$$\dot{\xi} = \xi[DF(s)] - dB\xi\Gamma. \tag{2}$$

In this expression, $DF(s) \in \mathbb{R}^{m\times m}$ denotes the Jacobian matrix of F evaluated at s, and $\xi = (\xi_1, \xi_2, \ldots, \xi_N)^T \in \mathbb{R}^{N\times m}$, where $\xi_i(t) = x_i(t) - s(t)$ for $i = 1, 2, \ldots, N$. Additionally, the matrix B is given by

$$B = \left(\frac{c}{d}L + E\right). \tag{3}$$

The matrix E is diagonal, with all diagonal elements set to 1 for driver nodes and 0 for non-driver nodes.

By projecting ξ onto the eigenvectors of the B matrix (so that $\lambda_i\varphi_i = B\varphi_i$) and expressing $\xi = \Phi\vartheta$ with $\Phi = [\varphi_1, \varphi_2, \ldots, \varphi_N] \in \mathbb{R}^{N\times N}$, the dynamics can be rewritten as

$$\dot{\vartheta} = \vartheta[DF(s)] - d\Delta\vartheta\Gamma, \tag{4}$$

where $\Delta = \mathrm{diag}(\lambda_1, \lambda_2, \ldots, \lambda_N)$. Thus, the temporal evolution of the ith component is described by

$$\dot{\vartheta}_i^T = [DF(s) - d\lambda_i\Gamma]\vartheta_i^T, \quad i = 1, 2, \ldots, N. \tag{5}$$

According to classical linear stability analysis, exponential convergence to the desired trajectory is guaranteed provided that the largest Lyapunov exponent of the variational system governed by $[DF(s) - d\lambda_1\Gamma]$ is negative. This condition can be reduced to the inequality $d\lambda_1 > \theta$, where λ_1 denotes the smallest eigenvalue of the matrix B and θ is the critical threshold required for stability. This condition is in complete agreement with the MSF framework and was formally derived by Wang and Chen.[40]

This criterion reveals that networks characterized by larger values of λ_1 require a smaller control gain to ensure stability. Consequently, the size of λ_1 serves as a key indicator of the effectiveness of the chosen driver nodes. For a fixed driver set, a greater λ_1 corresponds to a more favorable configuration.

B. Convergence analysis in pinning synchronization

The convergence rate characterizes how quickly the network trajectory approaches the reference state s from an arbitrary initial condition. To quantify this, define

$$\mu_i = \|\xi_i\|^2 = \xi_i^T\xi_i. \tag{6}$$

The normalized variation of μ_i can be expressed as

$$\frac{\dot{\mu}_i}{\mu_i} = \frac{\xi_i^T[DF(s)^T + DF(s)]\xi_i}{\|\xi_i\|^2} - 2c\lambda_i. \tag{7}$$

If the fluctuation component is negligible, the solution evolves approximately as

$$\mu_i(t) \approx \mu_i(0)e^{-2c\lambda_i t}, \tag{8}$$

implying a decay rate of $-2c\lambda_i$. As a result, the global convergence rate is governed by the quantity $\min_i 2c\lambda_i = 2c\lambda_1$. Hence, the smallest eigenvalue of matrix B directly specifies the asymptotic speed with which synchronization is achieved.[42]

C. First- and second-order perturbation theory

Perturbation theory offers a structured approach for examining how small alterations to a matrix influence its eigenvalues and eigenvectors. Consider a perturbed matrix of the form

$$A(\varepsilon) = A^0 + \varepsilon D, \tag{9}$$

where A^0 denotes the unperturbed matrix (e.g., the Laplacian of the network), D represents the perturbation matrix (e.g., diagonal modification corresponding to node selection), and ε is a small perturbation parameter. According to the classical perturbation theory, both eigenvalues and eigenvectors of $A(\varepsilon)$ can be expanded in a Taylor series around $\varepsilon = 0$,

$$\lambda(\varepsilon) = \lambda^0 + \varepsilon\lambda^{(1)} + \varepsilon^2\lambda^{(2)} + \mathcal{O}(\varepsilon^3), \tag{10}$$

$$v(\varepsilon) = v^0 + \varepsilon v^{(1)} + \varepsilon^2 v^{(2)} + \mathcal{O}(\varepsilon^3), \tag{11}$$

where λ^0 and v^0 denote the eigenvalue and eigenvector of the unperturbed system, respectively. It is notable that these perturbation expansions are valid under the assumption that λ^0 is a simple (non-degenerate) eigenvalue and the eigenvectors of A^0 are assumed to be orthonormal. Crucially, in this work, an augmented Laplacian matrix is considered, and the focus is specifically on estimating its smallest eigenvalue using perturbation expansions. While the general theory of perturbation expansions requires all eigenvalues to be simple, here, the objective is solely to approximate the smallest eigenvalue, λ_1. Therefore, the potential degeneracy of higher eigenvalues does not affect the approximation of λ_1, as their specific

28 September 2026 14:34:12

Published under an exclusive license by AIP Publishing

behavior is not critical to this analysis. Substituting these expansions into the eigenvalue equation

$$A(\varepsilon)v_i(\varepsilon) = \lambda_i(\varepsilon)v_i(\varepsilon) \tag{12}$$

and equating terms of equal order in ε, yields the perturbation relations. At the first order, the eigenvalue correction is given by

$$\lambda_i^{(1)} = \left(v_i^0\right)^T D v_i^0, \tag{13}$$

known as the first-order perturbation formula. Consequently, the perturbed eigenvalue can be approximated up to the first order as

$$\lambda_i(\varepsilon) \approx \lambda_i^0 + \varepsilon\left(v_i^0\right)^T D v_i^0. \tag{14}$$

This approximation is computationally inexpensive and already provides valuable insight into the sensitivity of eigenvalues with respect to perturbations, though higher-order terms are often required for improved accuracy.

To improve accuracy, the second-order correction is included, which takes the form

$$\lambda_i^{(2)} = \sum_{j\neq i} \frac{\left(\left(v_j^0\right)^T D v_i^0\right)^2}{\lambda_i^0 - \lambda_j^0}, \tag{15}$$

where the index i corresponds to the target eigenvalue, v_j^0 and λ_j^0 denote the eigenvector and eigenvalue associated with the jth mode, respectively. This formula is derived by solving the higher-order terms while enforcing the orthogonality conditions of eigenvectors. As a result, the second-order approximation of the eigenvalue is expressed as

$$\lambda_i(\varepsilon) \approx \lambda_i^0 + \varepsilon\left(v_i^0\right)^T D v_i^0 + \varepsilon^2 \sum_{j\neq i} \frac{\left(\left(v_j^0\right)^T D v_i^0\right)^2}{\lambda_i^0 - \lambda_j^0}. \tag{16}$$

This expression forms the theoretical foundation of the proposed method. By perturbing the diagonal entries of the Laplacian matrix and evaluating the approximate change in the smallest eigenvalue via the above formula, the contribution of each node to network controllability can be systematically quantified. In this work, the perturbation term ε represents the control gain assigned to individual driver nodes. Consequently, driver nodes are selected sequentially based on their ability to maximize the increase in $\lambda_1(\varepsilon)$. This theoretical framework naturally motivates the use of perturbation theory in this work, as it provides an efficient way to approximate the variations of λ_1 under small diagonal perturbations in L, thereby guiding the systematic identification of effective driver nodes for pinning control.

III. PROPOSED METHOD

The central idea of the proposed method is to employ a second-order perturbation expansion to approximate the smallest eigenvalue associated with the Laplacian matrix after sequentially selecting a set of driver nodes. At each step, let the current Laplacian be denoted by L, with the smallest eigenvalue λ_1 and associated eigenvector v_1. The corresponding eigensystem is written as $\{\lambda_j, v_j\}_{j=1}^N$.

When a set of k nodes is designated as drivers, the perturbation matrix D is defined as a diagonal matrix with entries equal to 1 for selected nodes and zero otherwise. The perturbed eigenvalue is then approximated as

$$\lambda_1(\varepsilon) \approx \lambda_1 + \varepsilon v_1^T D v_1 + \varepsilon^2 \sum_{j\neq 1} \frac{\left(v_j^T D v_1\right)^2}{\lambda_1 - \lambda_j}. \tag{17}$$

This formulation makes it possible to approximate the effect of adding each candidate node to the current driver set based on the current eigensystem, rather than performing a full eigendecomposition for all possible perturbations. In sequential selection, at each step, a node is selected that yields the largest incremental increase in λ_1.

The second-order perturbation framework is selected because, at each step of the sequential pinning procedure, evaluating a candidate driver node i is equivalent to assessing the spectral effect of a localized positive rank-one update to the current augmented Laplacian (L). For a simple smallest eigenvalue λ_1 of L, with normalized eigenvector v_1, the perturbation expansion in Eq. (17) consists of a first-order term, $\varepsilon v_1^T D v_1$, and a second-order term, $\varepsilon^2 \sum_{j\neq 1} \frac{(v_j^T D v_1)^2}{\lambda_1 - \lambda_j}$. The first-order contribution reflects only the direct participation of node i in the current critical eigenmode, whereas the second-order correction accounts for the coupling of this mode with the remaining eigenvectors through the inverse spectral separations $(\lambda_1 - \lambda_j)^{-1}$. It thus captures the leading global redistribution of spectral influence induced by the localized pinning action, which is essential for reliably ranking competing candidate nodes. Moreover, since $\lambda_j > \lambda_1$ for $j \neq 1$, this correction is non-positive and represents the curvature of the smallest-eigenvalue path under the perturbation. Hence, the second-order approximation provides the lowest-order computationally tractable model that incorporates intermodal effects while avoiding the repeated computation of the complete eigensystem for every candidate node, offering an appropriate balance between spectral accuracy, physical interpretability, and computational efficiency.

One inherent limitation of the perturbation method is that it requires the perturbations to remain sufficiently small. Specifically, the validity of the Taylor expansion and the truncation of higher-order terms can only be guaranteed when the perturbation amplitude is confined within a limited range.

It is worth emphasizing that the perturbation-based approach employed in this study achieves higher accuracy in identifying driver nodes in dense networks. This advantage can be explained by two spectral properties. First, in dense networks, the eigenvalues of the Laplacian (or adjacency) matrix are typically spread over a wider range, which means that a small local perturbation (e.g., modifying a diagonal entry) has a relatively smaller effect on the overall spectrum. Consequently, the fundamental condition for the convergence of the perturbation series—that the perturbation magnitude is much smaller than the spectral spacing—is better satisfied. Second, dense networks usually exhibit a larger spectral gap. Since the perturbation corrections involve denominators of the form $(\lambda_i - \lambda_j)$, a larger spectral separation suppresses the higher-order terms, leading to faster convergence and greater stability of the approximation. In

28 September 2026 14:34:12

Published under an exclusive license by AIP Publishing

contrast, sparse networks tend to have small spectral gaps, making higher-order corrections more significant and reducing the accuracy of the perturbative method.

A spectral criterion can be introduced to quantify the applicability of the perturbation method. Let $R = d/\Delta_{\min}$, where d represents the magnitude of the diagonal perturbation applied to the Laplacian, and $\Delta_{\min}$ denotes the smallest difference between the eigenvalue of interest and the remaining eigenvalues. Perturbative expansions remain accurate when $R \ll 1$, as this ensures that higher-order terms contribute minimally. Dense networks naturally tend to meet this condition because their Laplacian eigenvalues are more widely separated, yielding larger $\Delta_{\min}$. Therefore, the ratio R serves as a practical spectral measure that links network density to the expected reliability of perturbation-based driver-node selection.

The computational complexity of the proposed scheme can be analyzed and compared with the Sequential Greedy Node Selection algorithm, which serves as a widely used baseline for sequential driver-node selection methods. The sequential greedy node selection method relies on a step-by-step greedy strategy to maximize the smallest eigenvalue (λ_1) of the augmented Laplacian matrix ($L + D$). The process begins by testing each node in the network individually as a potential first driver; the node that produces the highest λ_1 is selected. Once the first driver is fixed, the algorithm repeats this evaluation for the remaining nodes to find the second driver, ensuring that the new selection maximizes the eigenvalue increase given the first driver is already in place. This iterative procedure continues sequentially: at each stage, the set of previously selected drivers remains fixed, and the next driver is chosen from the remaining candidates to yield the optimal λ_1. By systematically evaluating the direct spectral impact of every candidate at every step, this method provides a rigorous, exhaustive reference point for comparing other sequential approaches.

The complexity of the proposed method is evaluated as follows:

The proposed method relies on an initial eigen-decomposition of the modified Laplacian matrix, followed by an iterative evaluation of the influence of each candidate node using a second-order perturbation expansion. The computational cost of each component is detailed as follows:

1. **Initial eigen-decomposition:** At the beginning of the algorithm, the matrix $L + D$, where D encodes the previously selected driver nodes, is decomposed once to obtain its eigenvalues and eigenvectors. This operation has a well-known computational complexity of $\mathcal{O}(N^3)$.
2. **Perturbation-based evaluation of candidate nodes:** To select a driver node, the influence of each candidate on the smallest eigenvalue λ_1 is approximated using the second-order perturbation expansion [refer to Eq. (17)]. This procedure incurs a computational cost of $\mathcal{O}(N^2)$.
3. **Repetition over all selection steps:** Since one driver node is selected at each iteration and a total of N nodes must be examined, the entire selection process is repeated N times.

Thus, each iteration requires one eigen-decomposition of cost $\mathcal{O}(N^3)$ and a perturbation-based evaluation phase of cost $\mathcal{O}(N^2)$. Consequently, the overall complexity of the proposed method becomes

$$\mathcal{O}(N) \times \left(\mathcal{O}(N^2) + \mathcal{O}(N^3)\right) \approx \mathcal{O}(N^4). \tag{18}$$

It can be seen that the perturbation-based approach achieves a total computational complexity of $\mathcal{O}(N^4)$, making it significantly more scalable than classical greedy approaches, especially for medium- and large-scale networks.

The sequential greedy node selection method requires, at each iteration, modifying the diagonal element of $L + D$ for each candidate node and performing a full eigen-decomposition to evaluate the resulting smallest eigenvalue. It needs

1. **Evaluation of all candidates per iteration:** For each of the N candidate nodes, modifying the matrix and computing its leading eigenvalue via full eigen-decomposition requires $\mathcal{O}(N^3)$. Therefore, evaluating all candidates at a single iteration costs $\mathcal{O}(N) \times \mathcal{O}(N^3) = \mathcal{O}(N^4)$.
2. **Repetition over all selection steps:** Because this procedure must be repeated for all N driver node selections, the total computational cost becomes $\mathcal{O}(N) \times \mathcal{O}(N^4) = \mathcal{O}(N^5)$.

Thus, the sequential greedy algorithm exhibits a prohibitive computational complexity of $\mathcal{O}(N^5)$.

By replacing repeated full eigen-decompositions with a perturbation-based approximation, the proposed method reduces the computational cost from $\mathcal{O}(N^5)$ to $\mathcal{O}(N^4)$. This reduction in computational complexity significantly enhances practicality and scalability, enabling efficient analysis of medium- to large-scale networks where traditional greedy methods become computationally infeasible.

IV. RESULTS

To assess how well the proposed approach performs, it is applied to networks exhibiting a variety of topological forms, such as small-world, scale-free, and randomly connected architectures. In all simulations, the coupling strength and the control gain are fixed at 1.

Small-world networks based on the Watts–Strogatz construction are produced by first forming a regular ring lattice where every node links to its q closest neighbors, and then randomly rewiring each edge with a probability p.

The scale-free networks (the Barabási–Albert model) are constructed through preferential attachment, beginning with an initial set of b_0 fully connected nodes and subsequently adding new nodes, each linked to b existing nodes, where the likelihood of choosing a particular node grows in accordance with its degree. Random networks (the Erdős–Rényi model) are formed by independently establishing each possible edge with probability k.

The evaluation criterion is defined as the similarity between the driver-node sequences obtained by different strategies and the corresponding sequence produced by the sequential greedy node selection method (a commonly adopted benchmark among sequential approaches). For each network topology, the similarity percentage is computed as the number of selected driver nodes increases.

To better understand how the perturbation-based strategies behave, a direct comparison between the first-order and second-order formulations is carried out, with their outcomes displayed in

28 September 2026 14:34:12

Published under an exclusive license by AIP Publishing

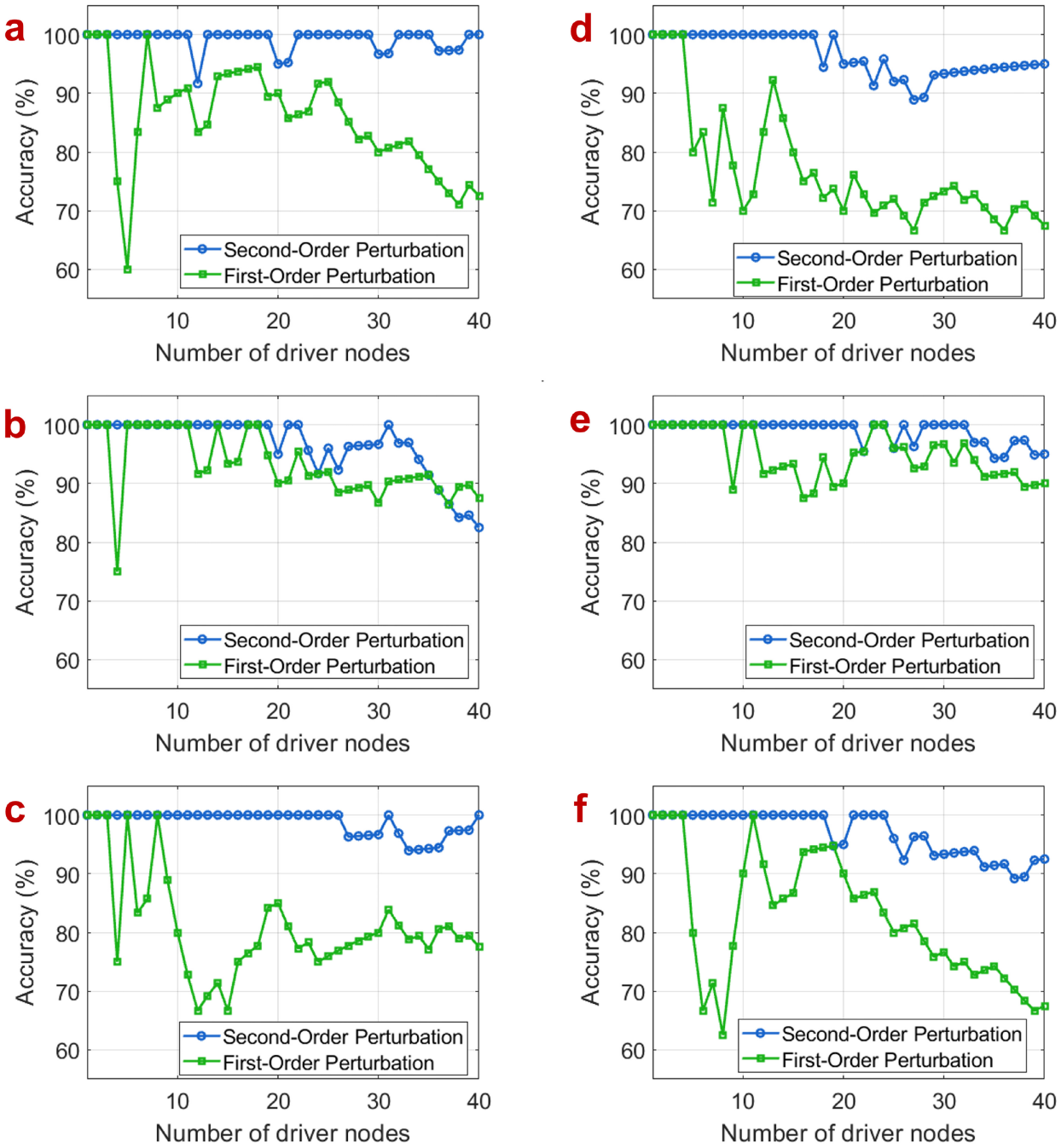


FIG. 1. Comparison of driver-node selection accuracy between first-order and second-order perturbation methods across six benchmark topologies: (a) a 100-node small-world network with parameters $q = 34$, $p = 0.8$; (b) a 100-node scale-free network with parameters $b_0 = 9$, $b = 8$; (c) a 100-node random network with parameter $k = 0.3$; (d) a 200-node small-world network with parameters $q = 20$, $p = 0.5$; (e) a 200-node scale-free network with parameters $b_0 = 6$, $b = 5$; and (f) a 200-node random network with parameter $k = 0.2$. Curves illustrate the selection accuracy (similarity relative to the sequential greedy benchmark) as a function of the number of chosen driver nodes for the second-order (blue curves) and first-order (green curves) approximations. The second-order perturbation method consistently achieves near-perfect accuracy across a wide range of driver-set sizes. In contrast, the first-order method exhibits strong fluctuations and lower accuracy, most prominently when the number of driver nodes grows. Because both formulations share the same asymptotic computational complexity of $\mathcal{O}(N^4)$, the second-order framework delivers substantial gains in fidelity without incurring additional computational overhead, establishing it as the superior tool for network-controllability assessment.

28 September 2026 14:34:12

Published under an exclusive license by AIP Publishing

Fig. 1. In these diagrams, the x-axis reports how many driver nodes have been chosen, whereas the y-axis reflects the similarity to the greedy benchmark. The blue curves represent the second-order perturbation method, and the green curves correspond to the first-order perturbation method.

As observed across all network topologies, the second-order perturbation method consistently maintains very high accuracy, often remaining at or near 100% similarity with the greedy benchmark for a broad range of driver-set sizes. This trend is evident in all cases, whether for small-world, scale-free, or random networks, underscoring the robustness of the second-order formulation. In contrast, the first-order method exhibits strong fluctuations, and the reliability of the method drops noticeably as more driver nodes are included. The superiority of the second-order perturbation method arises from its more accurate approximation of eigenvalue variations, which enables it to capture the influence of node selection on network controllability more faithfully.

Importantly, the computational burden of the first-order and second-order approaches is essentially comparable: while the first-order method has a complexity of $\mathcal{O}(N^4)$, the second-order method, as derived earlier, also scales as $\mathcal{O}(N^4)$. Thus, the substantial improvement in accuracy delivered by the second-order method comes at no extra computational cost.

Based on these findings, the second-order perturbation framework is adopted for subsequent analyses. It not only offers scalability suitable for large networks but also delivers results that remain consistently close to the greedy benchmark, thereby providing a practical and theoretically grounded tool for controllability analysis.

To further validate the reliability of the second-order perturbation framework, additional experiments are performed by averaging the accuracy results over a large number of independently generated networks. The purpose of this analysis is to ensure that the high similarity with the greedy benchmark, observed in individual networks, is not an artifact of a specific topology instance but a consistent property across an ensemble of independently generated networks. Specifically, for each topology type, multiple network realizations are constructed, and the corresponding accuracy curves of the second-order perturbation method are computed. The mean accuracy values, together with standard-deviation bounds, are then plotted as a function of the number of selected driver nodes, thereby providing a more comprehensive statistical assessment.

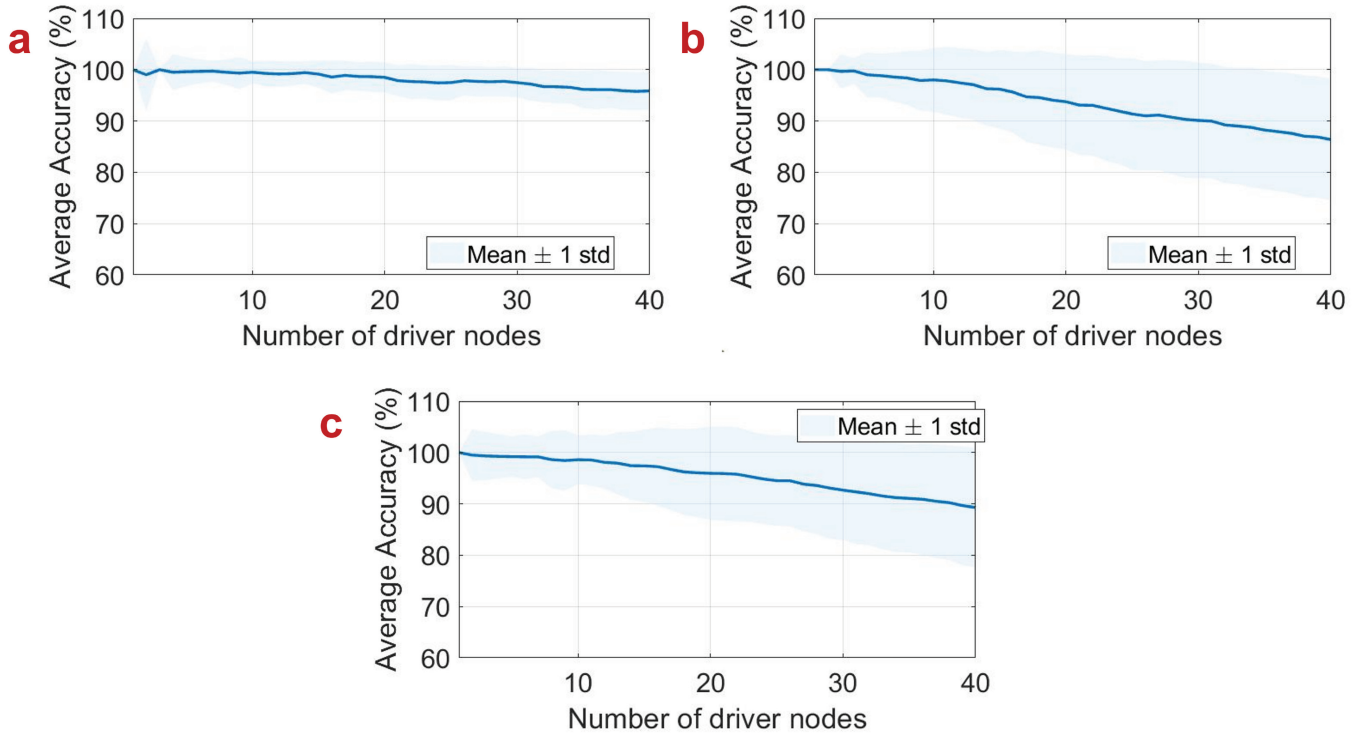


FIG. 2. Statistical evaluation and generalization performance of the second-order perturbation method across 100 independently generated network realizations for three distinct topologies ($N = 200$ nodes): (a) small-world networks ($q = 30$, $p = 0.7$); (b) scale-free networks ($b_0 = 8$, $b = 7$); and (c) Erdős–Rényi random networks ($k = 0.3$). Solid curves and shaded regions depict the ensemble mean accuracy and the corresponding ± 1 standard-deviation bounds, respectively, as a function of the number of selected driver nodes. The proposed framework consistently maintains high average accuracy—closely matching the greedy benchmark—across a wide range of driver-set sizes in all topological regimes. The narrow standard-deviation bands, particularly pronounced in scale-free topologies, demonstrate the robustness and stability of the method against structural randomness, confirming that its superior controllability performance is an intrinsic property rather than an artifact of specific network instances.

28 September 2026 14:34:12

Published under an exclusive license by AIP Publishing

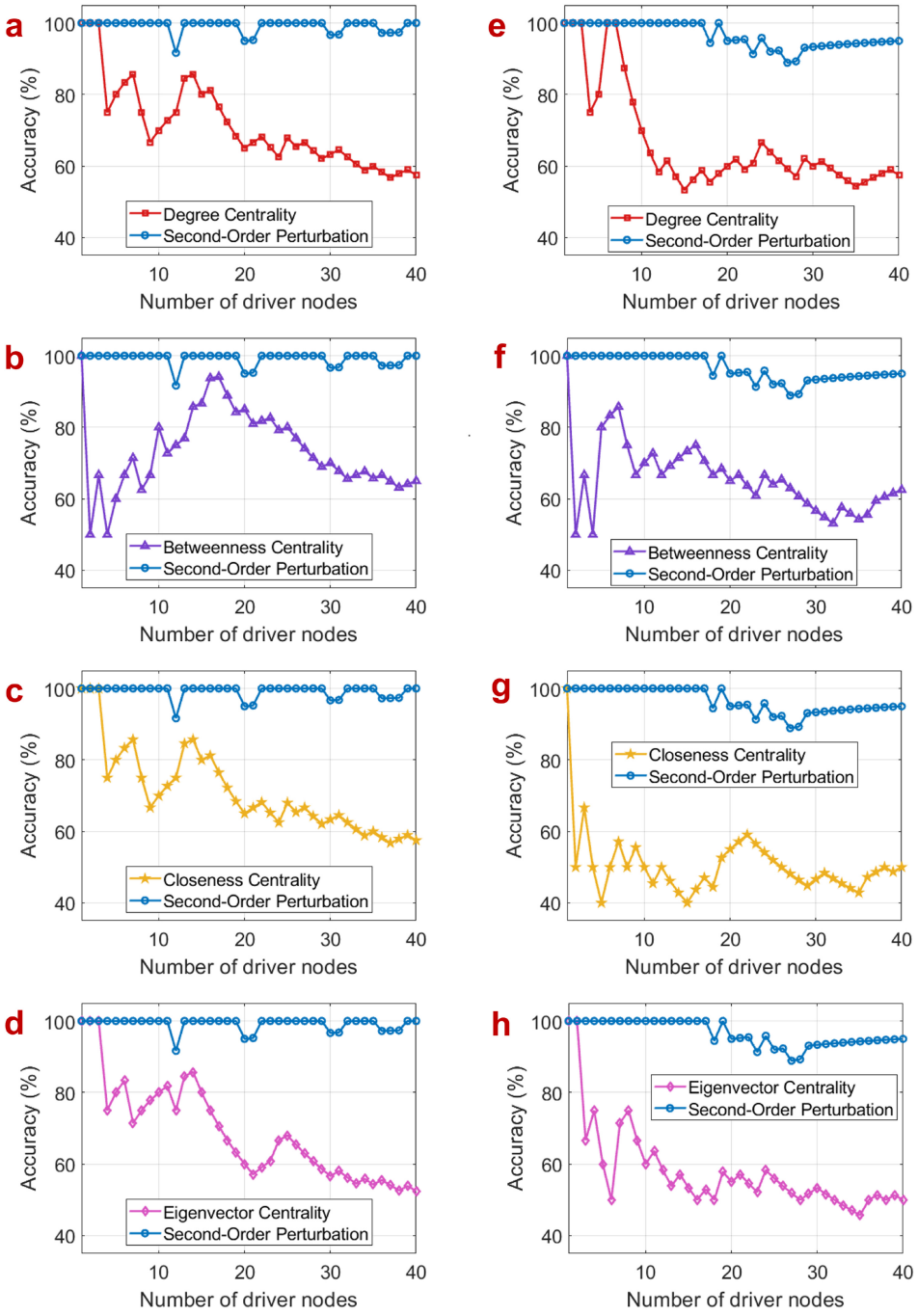


FIG. 3. Accuracy comparison between the second-order perturbation method and four centrality-based strategies for identifying driver nodes in small-world networks. The *x*-axis represents the number of selected driver nodes, and the *y*-axis shows the similarity of the selected driver set to the greedy benchmark, expressed as accuracy. Panels (a)–(d) present the results for the 100-node small-world network with $q = 34$ and $p = 0.8$, where (a) corresponds to degree centrality; (b) to betweenness centrality; (c) to closeness centrality; and (d) to eigenvector centrality. Panels (e)–(h) present the corresponding results for the 200-node small-world network with $q = 20$ and $p = 0.5$, where (e) corresponds to degree centrality; (f) to betweenness centrality; (g) to closeness centrality; and (h) to eigenvector centrality. Across all network configurations and driver-set sizes, the second-order perturbation method consistently achieves near-perfect or high and stable accuracy, reaching or closely approaching 100% in a substantial portion of the selection process. In contrast, the conventional centrality-based strategies exhibit pronounced fluctuations and generally lower agreement with the greedy benchmark. These discrepancies are particularly evident for closeness and eigenvector centrality, indicating that conventional centrality measures may not adequately capture the collective network-controllability structure. Consequently, they may lead to suboptimal driver-node configurations, whereas the second-order perturbation method provides a more reliable and robust approximation to the greedy driver-node selection strategy.

The results, summarized in dedicated figures for small-world, scale-free, and random networks (Fig. 2), demonstrate that the second-order perturbation method consistently achieves high average accuracies across a broad range of driver-set sizes. The relatively narrow standard-deviation bands—particularly in the scale-free case, and moderately in the small-world and random ensembles—confirm the robustness of the method, indicating that performance remains stable under structural variations.

These findings provide strong evidence that the proposed approach not only performs well in individual cases but also generalizes reliably to large ensembles, reinforcing its suitability for

28 September 2026 14:34:12

Published under an exclusive license by AIP Publishing

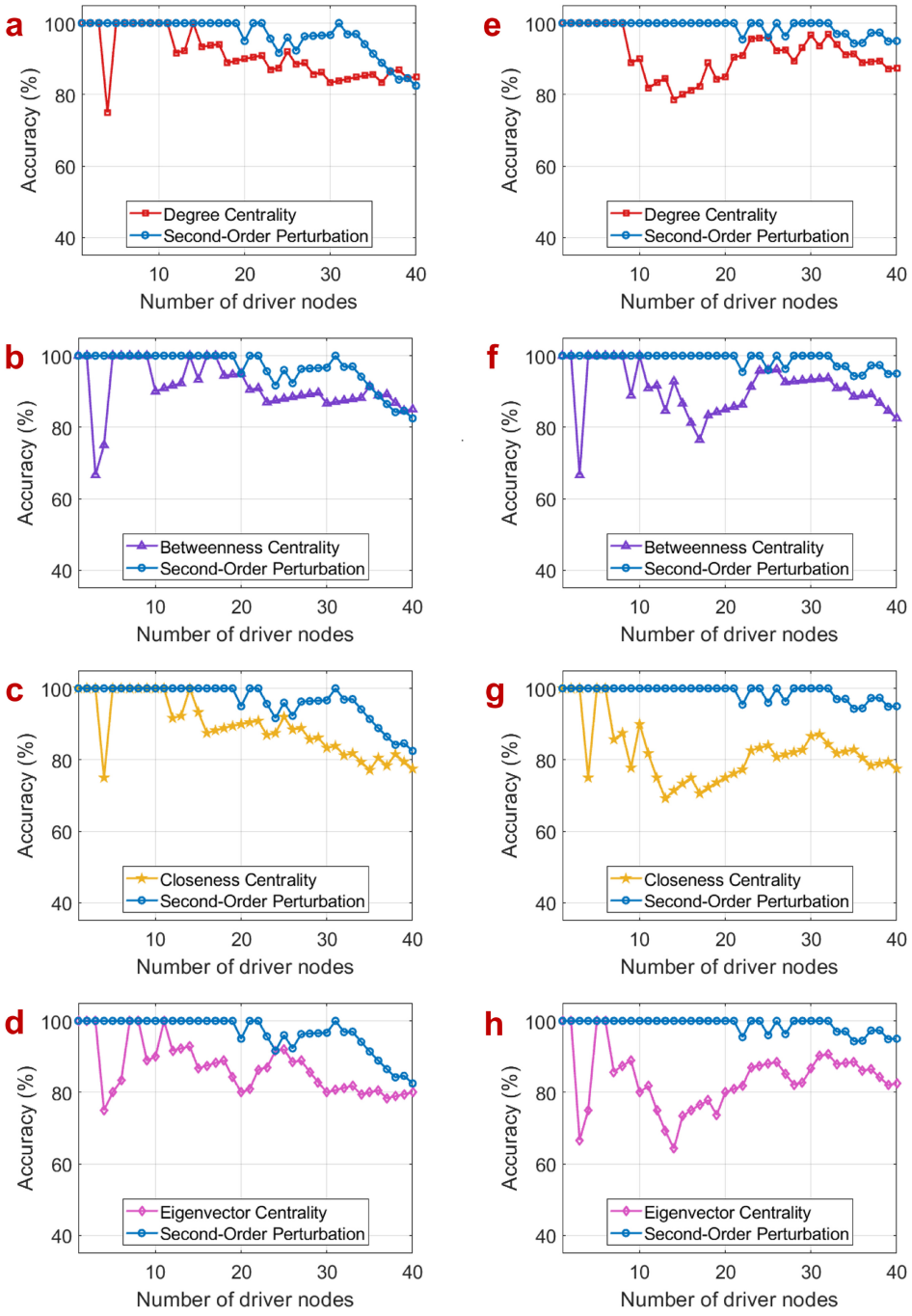


FIG. 4. Comparison of accuracy between the second-order perturbation method and four centrality-based strategies for identifying driver nodes in scale-free networks. The number of selected driver nodes is reported on the x-axis, while their similarity to the greedy benchmark is depicted on the y-axis as accuracy. Panels (a)–(d) present the results for the 100-node scale-free network with parameters $b_0 = 9$ and $b = 8$, where (a) corresponds to degree centrality; (b) to betweenness centrality; (c) to closeness centrality; and (d) to eigenvector centrality. Panels (e)–(h) present the corresponding results for the 200-node scale-free network with parameters $b_0 = 6$ and $b = 5$, where (e) corresponds to degree centrality; (f) to betweenness centrality; (g) to closeness centrality; and (h) to eigenvector centrality. Due to the structural heterogeneity and the presence of prominent hub nodes inherent to scale-free topologies, centrality metrics achieve a higher baseline accuracy compared to small-world and random networks, particularly for small driver-set sizes where they become comparable to the second-order perturbation method by exhibiting near-100% accuracy. However, as the driver set expands, these heuristic centrality measures rapidly deteriorate. In contrast, the second-order perturbation framework consistently maintains top-ranked performance and superior, near-optimal accuracy throughout the entire selection process across all driver-set sizes, highlighting its scalability, precision, and robust capacity to capture spectral shifts beyond hub-dominated dynamics in heterogeneous network architectures.

practical applications in controllability assessment of complex networks.

To complement the perturbation method analysis, additional experiments are conducted to compare the proposed second-order perturbation framework with four widely used centrality-based strategies—degree, betweenness, closeness, and eigenvector centrality—across all six network topologies under study (in Fig. 1). In each case, the accuracy of the driver-node sequences produced by these methods is evaluated relative to the greedy benchmark as the number of selected nodes increases.

28 September 2026 14:34:12

Published under an exclusive license by AIP Publishing

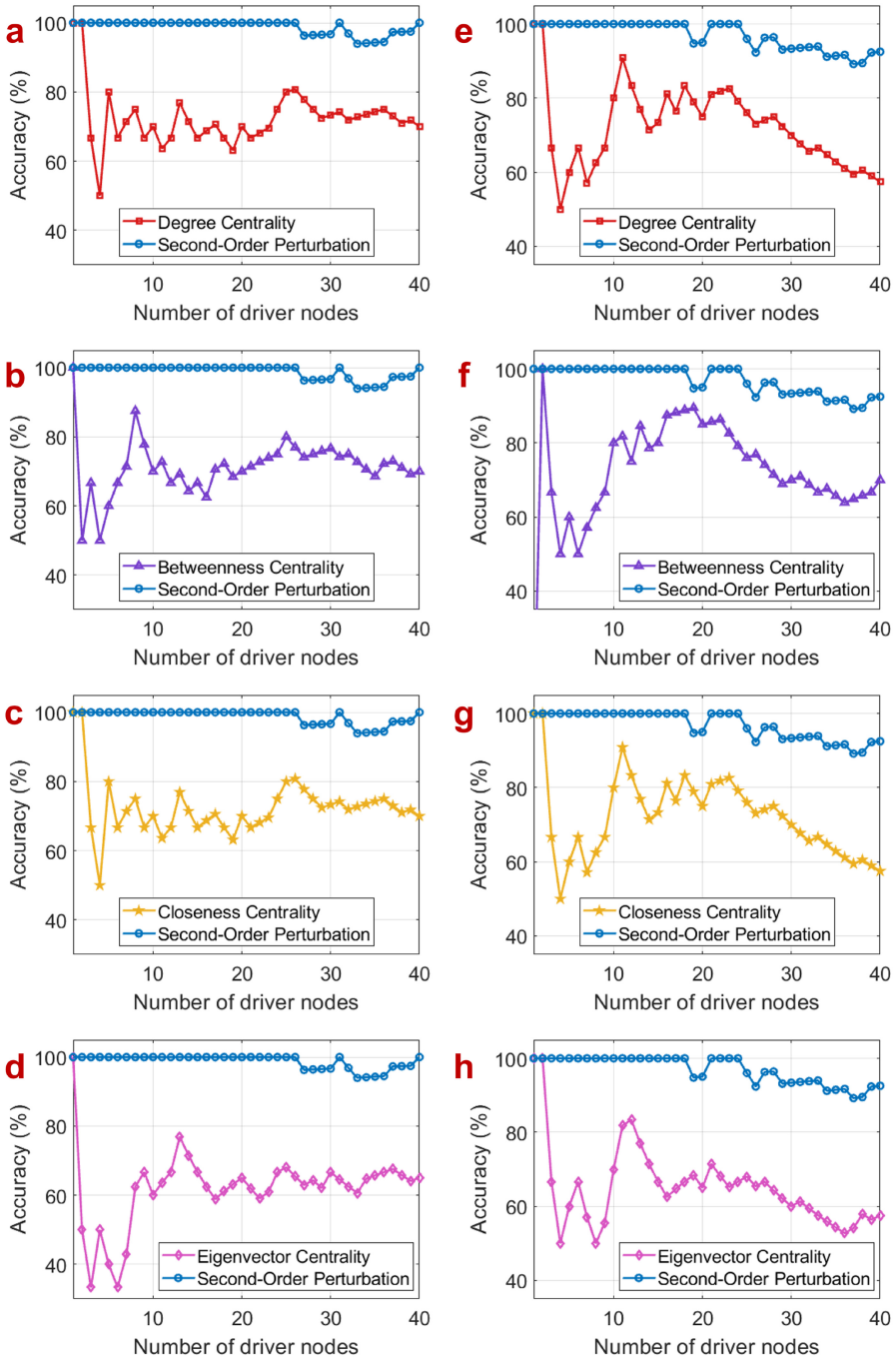


FIG. 5. Evaluation of driver-node identification accuracy using the second-order perturbation method alongside four centrality-based strategies in random networks. The *x*-axis indicates the count of chosen driver nodes, and the *y*-axis plots their similarity percentage relative to the greedy benchmark. Panels (a)–(d) display the results for the 100-node random network with connection probability $k = 0.3$, where (a) corresponds to degree centrality; (b) to betweenness centrality; (c) to closeness centrality; and (d) to eigenvector centrality. Panels (e)–(h) show the corresponding outcomes for the 200-node random network with $k = 0.2$, where (e) corresponds to degree centrality; (f) to betweenness centrality; (g) to closeness centrality; and (h) to eigenvector centrality. In homogeneous and sparse random topologies that lack pronounced hub hierarchies, centrality-based approaches struggle significantly, exhibiting performance degradation and erratic fluctuations. In contrast, the second-order perturbation framework demonstrates clear superiority and consistently outperforms all four heuristics by yielding driver node configurations that closely align with the optimal greedy benchmark, underscoring the advantage of incorporating the spectral properties of the *B* matrix over purely topological indicators.

The results, presented in Figs. 3–5, consistently show that none of the centrality-based approaches achieves accuracy levels comparable to the second-order perturbation method. In scale-free networks, degree centrality often performs reasonably well when a small number of driver nodes is required, reflecting the intuitive importance of high-degree hubs. However, its accuracy quickly deteriorates as the driver-set size increases. Betweenness, closeness, and eigenvector centrality display even greater variability, producing highly fluctuating curves that frequently deviate from the greedy reference. In contrast, the second-order perturbation method maintains consistently superior performance in most network configurations and across a broad range of driver-set sizes. These findings

28 September 2026 14:34:12

Published under an exclusive license by AIP Publishing

confirm that centrality measures are not sufficiently sensitive to capture the nuanced role of nodes in network controllability. The perturbation framework, by explicitly incorporating the spectral properties of the B matrix and approximating eigenvalue variations, provides a more principled and robust basis for node selection. Overall, the comparative analysis underscores the practical value of the proposed method, demonstrating that it consistently outperforms centrality-based heuristics and delivers results much closer to the greedy benchmark.

V. DISCUSSION

To further investigate the performance and robustness of the proposed method, a sensitivity analysis was conducted with respect to the control gain d. As mentioned before, one of the limitations associated with the proposed method is that the control gain must be sufficiently small. To thoroughly assess its impact, the resulting error is quantified as d increases. The sensitivity analysis is carried out by systematically increasing the value of d from 1 to 15. For each value of d, the smallest eigenvalue λ_1 is computed under both the perturbation-based strategy and the Sequential Greedy Selection method, for driver-set sizes ranging from 1 to $K_{\max}$. The error is quantified as the average percentage difference between the λ_1 values obtained using the two methods over driver-set sizes ranging from 1 to $K_{\max}$. It is calculated using the following formula:

$$\text{Error}(d) = \frac{1}{K_{\max}} \sum_{j=1}^{K_{\max}} \frac{100 \left| \lambda_1^{\text{Pert}_2}(j,d) - \lambda_1^{\text{Greedy}}(j,d) \right|}{\lambda_1^{\text{Greedy}}(j,d)}, \tag{19}$$

allowing a direct assessment of how the gain magnitude influences the accuracy of the perturbation-based approximation. The corresponding result for a random network comprising 100 nodes with $k = 0.4$ and $K_{\max} = 40$ is illustrated in Fig. 6. This graphical representation facilitates an understanding of the trade-off between the magnitude of the control gain and the accuracy of the perturbation-based eigenvalue estimation.

As the figure indicates, increasing d leads to a gradual rise in the approximation error, reflecting the natural limitations of second-order perturbation expansions when the control input becomes large. Nonetheless, for values up to approximately $d = 10$, the error remains relatively contained—about 10%—demonstrating that the perturbation-based approach retains strong fidelity to the greedy baseline within a practically meaningful range of gain values.

This behavior highlights the effectiveness of the proposed method under moderate control intensities and confirms that its predictive accuracy remains reliable across a broad and operationally relevant parameter regime.

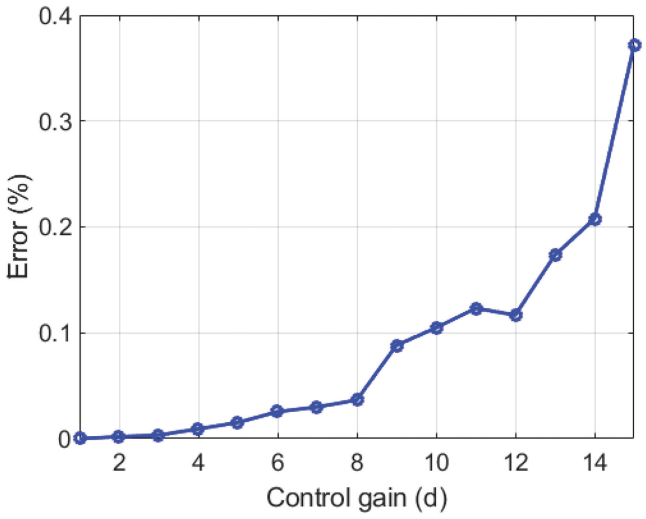


FIG. 6. Sensitivity analysis of the second-order perturbation framework with respect to the control gain d for an Erdős–Rényi random network ($N = 100$, $k = 0.4$). The plot shows the mean percentage error in approximating the smallest eigenvalue λ_1 relative to the greedy baseline [evaluated via Eq. (19)] as d increases from 1 to 15. As expected from asymptotic expansions, the approximation error grows monotonically with increasing control gain. However, the error remains well-contained below approximately 10% for gains up to $d \approx 10$. This demonstrates that the proposed perturbation framework maintains high fidelity and predictive accuracy over a broad, operationally relevant range of control intensities before higher-order nonlinear effects become dominant.

VI. CONCLUSION

In this study, we investigated the driver-node selection problem for pinning controllability in complex dynamical networks and introduced an analytical second-order perturbation framework. By approximating the shift in the smallest non-zero eigenvalue of the grounded Laplacian matrix under diagonal modifications, the proposed method provides a principled criterion for ranking candidate pinning nodes without requiring exhaustive combinatorial evaluations. Computationally, the framework reduces the complexity from $\mathcal{O}(N^5)$ for the standard sequential greedy procedure to $\mathcal{O}(N^4)$, while preserving near-optimal selection accuracy across different network sizes and topological classes.

First, despite sharing the same asymptotic complexity of $\mathcal{O}(N^4)$, the first- and second-order formulations exhibit substantially different selection performances. The first-order approximation shows noticeable degradation and fluctuations as the number of selected driver nodes increases, whereas the second-order method retains near-100% fidelity relative to the sequential greedy benchmark over a broad range of driver set sizes. This result demonstrates the importance of incorporating second-order perturbation corrections for reliable driver-node ranking. Second, statistical evaluations over 100 independently generated realizations of small-world, scale-free, and Erdős–Rényi random networks show that the proposed method maintains high mean accuracy and closely matches the greedy benchmark across a wide range of driver-set sizes. Moreover, the narrow standard-deviation bands observed across the ensembles—particularly for the scale-free networks—indicate limited sensitivity to structural randomness. These findings confirm that the favorable performance of the proposed approach is not restricted to individual network instances but persists across independently generated networks with the same underlying topology. Third, across small-world, scale-free, and Erdős–Rényi random networks, the

28 September 2026 14:34:12

Published under an exclusive license by AIP Publishing

proposed framework outperforms the degree, betweenness, closeness, and eigenvector centrality heuristics. Although the presence of structural hubs in scale-free networks provides centrality-based strategies with a relatively higher baseline accuracy, closeness and eigenvector centralities tend to exhibit comparatively larger deviations from the greedy benchmark in several scenarios. In contrast, the second-order method consistently achieves near-optimal and robust accuracy across the considered topological regimes, including networks with different edge densities and degrees of structural heterogeneity. Finally, the sensitivity analysis with respect to the feedback control gain d further supports the practical reliability of the method. Specifically, the mean percentage approximation error remains below approximately 10% for moderate gain values ($d \approx 10$), indicating that the proposed approximation remains effective over a practically relevant range of control gains.

Overall, these quantitative and qualitative findings show that the second-order perturbation strategy provides a favorable balance between spectral accuracy and computational scalability, thereby making it particularly suitable for large-scale networked systems in which exhaustive or sequential greedy searches become computationally impractical. Future work may extend the present framework to adaptive and time-varying pinning strategies, weighted, directed, and multilayer networks, as well as systems with heterogeneous node dynamics, actuator constraints, and uncertainty in network structure or control gains. Further directions include the joint optimization of driver-node locations and pinning strengths, together with robustness-oriented formulations incorporating additional control objectives beyond stabilization.

ACKNOWLEDGMENTS

M.P. was supported by the Slovenian Research and Innovation Agency (Javna agencija za znanstvenoraziskovalno in inovacijsko dejavnost Republike Slovenije) (Grant No. P1-0403).

AUTHOR DECLARATIONS

Conflict of Interest

The authors have no conflicts to disclose.

Author Contributions

Fatemeh Ghoreishian Amiri: Conceptualization (equal); Methodology (lead); Writing – original draft (lead). **Fahimeh Nazarimehr:** Conceptualization (equal); Supervision (equal); Writing – review & editing (equal). **Sajad Jafari:** Supervision (supporting); Validation (lead); Writing – review & editing (equal). **Matjaž Perc:** Supervision (equal); Validation (equal); Writing – review & editing (equal).

DATA AVAILABILITY

The data generated during the current study are available from the corresponding author upon reasonable request.

REFERENCES

[1]Y.-Y. Liu, J.-J. Slotine, and A.-L. Barabasi, "Controllability of complex networks," Nature **473**, 167–73 (2011).
[2]G. Yan, G. Tsekenis, B. Barzel, J.-J. Slotine, Y.-Y. Liu, and A.-L. Barabasi, "Spectrum of controlling and observing complex networks," Nat. Phys. **11**, 779–786 (2015).
[3]C. Hens, U. Harush, S. Haber, R. Cohen, and B. Barzel, "Spatiotemporal signal propagation in complex networks," Nat. Phys. **15**, 403–412 (2019).
[4]H. Liu, X. Xu, J. A. Lu, G. Chen, and Z. Zeng, "Optimizing pinning control of complex dynamical networks based on spectral properties of grounded laplacian matrices," IEEE Trans. Syst. Man Cybern.: Syst. **51**, 786–796 (2021).
[5]Z. Cheng, Y. Xin, J. Cao, X. Yu, and G. Lu, "Selecting pinning nodes to control complex networked systems," Sci. China Technol. Sci. **61**, 1537–1545 (2018).
[6]J. Lu, D. Ho, and Z. Wang, "Pinning stabilization of linearly coupled stochastic neural networks via minimum number of controllers," IEEE Trans. Neural Networks **20**, 1617–1629 (2009).
[7]A. Haber, F. Molnár, and A. Motter, "State observation and sensor selection for nonlinear networks," IEEE Trans. Control Network Syst. **5**, 694–708 (2017).
[8]A. Vinayagam, T. E. Gibson, H.-J. Lee, B. Yilmazel, C. Roesel, Y. Hu, Y. Kwon, A. Sharma, Y.-Y. Liu, N. Perrimon, and A.-L. Barabási, "Controllability analysis of the directed human protein interaction network identifies disease genes and drug targets," Proc. Natl. Acad. Sci. U.S.A. **113**, 4976–4981 (2016).
[9]M. Doostmohammadian and U. A. Khan, "Graph-theoretic distributed inference in social networks," IEEE J. Sel. Top. Signal Process. **8**, 613–623 (2014).
[10]X.-D. Gao, W.-X. Wang, and Y.-C. Lai, "Control efficacy of complex networks," Sci. Rep. **6**, 28037 (2016).
[11]S. Pequito, S. Kar, and A. P. Aguiar, "Minimum number of information gatherers to ensure full observability of a dynamic social network: A structural systems approach," in *2014 IEEE Global Conference on Signal and Information Processing (GlobalSIP)* (IEEE, 2014), pp. 750–753.
[12]Y. Hu, D. Yu, T. Li, Y. Wu, Q. Ding, and Y. Jia, "Effect of spatial-phase drift on the synchronization of swarmalators with higher-order interactions," Commun. Phys. **8**, 177 (2025).
[13]S. Majhi, S. Ghosh, P. K. Pal, S. Pal, T. K. Pal, D. Ghosh, J. Završnik, and M. Perc, "Patterns of neuronal synchrony in higher-order networks," Phys. Life Rev. **52**, 144–170 (2025).
[14]I. Franović, K. Todorović, N. Vasović, and N. Burić, "Cluster synchronization of spiking induced by noise and interaction delays in homogenous neuronal ensembles," Chaos **22**, 033147 (2012).
[15]I. Franović and V. Miljković, "Functional motifs: A novel perspective on burst synchronization and regularization of neurons coupled via delayed inhibitory synapses," Chaos, Solitons Fractals **44**, 122–130 (2011).
[16]A. Mishra, S. Saha, S. Ghosh, S. K. Dana, and C. Hens, "Contrarian role of phase and phase velocity coupling in synchrony of second-order phase oscillators," Phys. Rev. E **108**, L042201 (2023).
[17]S. Acharya, G. K. Sar, S. Samanta, D. Ghosh, and S. K. Bhowmick, "Distance synchrony in coupled systems," Chaos, Solitons Fractals **187**, 115347 (2024).
[18]D. Xu, C. Dai, H. Su, and Y. Liu, "Synchronization analysis for delayed multilinked large-scale networks via intermittent delayed event-triggered control," IEEE Trans. Control Network Syst. **12**, 2676–2688 (2025).
[19]Z. Ye, Y. Wu, Q. Ding, Y. Xie, and Y. Jia, "Finding synchronization state of higher-order motif networks by dynamic learning," Phys. Rev. Res. **6**, 033071 (2024).
[20]Y. Wu, Q. ding, W. Huang, L. Tianyu, D. Yu, and Y. Jia, "Dynamic learning of synchronization in coupled nonlinear systems," Nonlinear Dyn. **112**, 21945–21967 (2024).
[21]S. Panahi, F. Nazarimehr, S. Jafari, J. C. Sprott, M. Perc, and R. Repnik, "Optimal synchronization of circulant and non-circulant oscillators," Appl. Math. Comput. **394**, 125830 (2021).
[22]Q. Ding, Y. Wu, W. Huang, and Y. Jia, "A dynamic learning method for phase synchronization control in Hodgkin–Huxley neuronal networks," Eur. Phys. J. Spec. Top. **234**, 2789–2802 (2025).
[23]S. Majhi, D. Ghosh, and J. Kurths, "Emergence of synchronization in multiplex networks of mobile Rössler oscillators," Phys. Rev. E **99**, 012308 (2019).
[24]Y. Wang, J. Lu, J. Liang, J. Cao, and M. Perc, "Pinning synchronization of nonlinear coupled lur'e networks under hybrid impulses," IEEE Trans. Circuits Syst. II: Express Briefs **66**(3), 432–436 (2019).

28 September 2026 14:34:12

Published under an exclusive license by AIP Publishing

[25]M. Chen, X. Luo, Y. Zhang, H. Wu, Q. Xu, and B. Bao, "Initial-boosted behaviors and synchronization of memristor-coupled memristive systems," IEEE Trans. Circuits Syst. I Regul. Pap. **71**, 781–793 (2024).
[26]Y. Xiao, S. Zhang, and L. Wang, "Synchronization of stochastic networked systems via nonlinear distributed control," IEEE Trans. Control Network Syst. **13**, 786–796 (2026).
[27]C. Meena, C. Hens, S. Acharyya, S. Haber, S. Boccaletti, and B. Barzel, "Emergent stability in complex network dynamics," Nat. Phys. **19**, 1033–1042 (2023).
[28]E. Yildirim and T. Yucelen, "Control of multiagent networks with misbehaving nodes over directed graph topologies," IEEE Trans. Control Network Syst. **12**, 1521–1530 (2025).
[29]F. Pasqualetti, S. Zampieri, and F. Bullo, "Controllability metrics, limitations and algorithms for complex networks," IEEE Trans. Control Network Syst. **1**, 40–52 (2014).
[30]X. Li, G. Li, L. Gao, L. Y. Chew, and G. Xiao, "Structural controllability of multiplex networks with the minimum number of driver nodes," IEEE Trans. Control Network Syst. **11**, 2088–2100 (2024).
[31]J. Liu, Z. Wu, Q. Xin, M. Yu, and L. Liu, "Topology uniformity pinning control for multi-agent flocking," Complex Intell. Syst. **10**, 2013–2027 (2024).
[32]A. Y. Alanis, J. Hernandez-Barragan, D. Ríos-Rivera, O. D. Sanchez, and G. Martinez-Soltero, "Constrained binary optimization approach for pinned node selection in pinning control of complex dynamical networks," Axioms **12**, 1088 (2023).
[33]A. M. Amani, M. Jalili, X. Yu, and L. Stone, "Controllability of complex networks: Choosing the best driver set," Phys. Rev. E **98**, 030302 (2018).
[34]Y. Zhang, A. Garas, and F. Schweitzer, "Control contribution identifies top driver nodes in complex networks," Adv. Complex Syst. **22**, 1950014 (2019).
[35]T. Qin, G. Duan, and A. Li, "Detecting the driver nodes of temporal networks," New J. Phys. **25**, 083031 (2023).
[36]W. Bomela, M. Sebek, R. Nagao, B. Singhal, I. Kiss, and J.-S. Li, "Finding influential nodes in networks using pinning control: Centrality measures confirmed with electrochemical oscillators," Chaos **33**, 093128 (2023).
[37]G. Zhang, Z. Liu, X. Yu, and M. Jalili, "Identifying the most influential driver nodes for pinning control of multi-agent systems with time-varying topology," arXiv:2405.18712 (2024).
[38]H. Liu, B.-J. Wang, J.-A. Lu, and Z.-Y. Li, "Node-set importance and optimization algorithm of nodes selection in complex networks based on pinning control," Acta Phys. Sin. **70**, 056401 (2021).
[39]X. Zhou, R. Wang, W. Li, and Z. Zhang, "Maximizing the smallest eigenvalue of grounded laplacian matrix," J. Global Optim. **91**, 807–828 (2025).
[40]X. F. Wang and G. Chen, "Pinning control of scale-free dynamical networks," Physica A **310**, 521–531 (2002).
[41]X. Li, X. Wang, and G. Chen, "Pinning a complex dynamical network to its equilibrium," IEEE Trans. Circuits Syst. I Regul. Pap. **51**, 2074–2087 (2004).
[42]Z. Mao, T. Fan, and L. Lü, "Perturbation-based pinning control strategy for enhanced synchronization in complex networks," IEEE Trans. Syst. Man Cybern.: Syst. **56**, 3328–3339 (2026).

28 September 2026 14:34:12

Published under an exclusive license by AIP Publishing